

2015

# Copepod carcasses as microbial hot spots for pelagic denitrification

RN Glud

HP Grossart

M Larsen

KW Tang

*Virginia Institute of Marine Science*

KE Arendt

*See next page for additional authors*

Follow this and additional works at: <https://scholarworks.wm.edu/vimsarticles>



Part of the [Aquaculture and Fisheries Commons](#)

---

## Recommended Citation

Glud, RN; Grossart, HP; Larsen, M; Tang, KW; Arendt, KE; and Et al., "Copepod carcasses as microbial hot spots for pelagic denitrification" (2015). *VIMS Articles*. 824.

<https://scholarworks.wm.edu/vimsarticles/824>

---

**Authors**

RN Glud, HP Grossart, M Larsen, KW Tang, KE Arendt, and Et al.

## Copepod carcasses as microbial hot spots for pelagic denitrification

Ronnie N. Glud,<sup>\*1,2,3,4</sup> Hans-Peter Grossart,<sup>5,6</sup> Morten Larsen,<sup>1,2</sup> Kam W. Tang,<sup>7,8</sup> Kristine E. Arendt,<sup>3</sup> Søren Rysgaard,<sup>3,4,9</sup> Bo Thamdrup,<sup>1</sup> Torkel Gissel Nielsen<sup>10</sup>

<sup>1</sup>Nordic Centre for Earth Evolution, Department of Biology, University of Southern Denmark, Odense M, Denmark

<sup>2</sup>Scottish Association for Marine Science, Scottish Marine Institute, Group for Biogeochemistry Oban, United Kingdom

<sup>3</sup>Greenland Climate Research Centre, Greenland Institute of Natural Resources, Nuuk, Greenland

<sup>4</sup>Arctic Research Centre, University of Aarhus, Aarhus, Denmark

<sup>5</sup>Leibniz-Institute of Freshwater Ecology and Inland Fisheries, Stechlin, Germany

<sup>6</sup>Institute for Biochemistry and Biology, Potsdam University, Potsdam, Germany

<sup>7</sup>Virginia Institute of Marine Science, College of William & Mary, Gloucester Point, Virginia

<sup>8</sup>Department of Biosciences and Centre for Sustainable Aquatic Research (CSAR), Swansea University, Swansea, United Kingdom

<sup>9</sup>Department of Geological Sciences and Centre for Earth Observation Science, University of Manitoba, Winnipeg, Manitoba, Canada

<sup>10</sup>Technical University of Denmark, DTU-Aqua, Charlottenlund, Denmark

### Abstract

Copepods are exposed to a high non-predatory mortality and their decomposing carcasses act as micro-niches with intensified microbial activity. Sinking carcasses could thereby represent anoxic microenvironment sustaining anaerobic microbial pathways in otherwise oxic water columns. Using non-invasive O<sub>2</sub> imaging, we document that carcasses of *Calanus finmarchicus* had an anoxic interior even at fully air-saturated ambient O<sub>2</sub> level. The extent of anoxia gradually expanded with decreasing ambient O<sub>2</sub> levels. Concurrent microbial sampling showed the expression of nitrite reductase genes (*nirS*) in all investigated carcass samples and thereby documented the potential for microbial denitrification in carcasses. The *nirS* gene was occasionally expressed in live copepods, but not as consistently as in carcasses. Incubations of sinking carcasses in <sup>15</sup>NO<sub>3</sub><sup>-</sup> amended seawater demonstrated denitrification, of which on average 34% ± 17% (*n* = 28) was sustained by nitrification. However, the activity was highly variable and was strongly dependent on the ambient O<sub>2</sub> levels. While denitrification was present even at air-saturation (302 μmol L<sup>-1</sup>), the average carcass specific activity increased several orders of magnitude to ~ 1 nmol d<sup>-1</sup> at 20% air-saturation (55 μmol O<sub>2</sub> L<sup>-1</sup>) at an ambient temperature of 7°C. Sinking carcasses of *C. finmarchicus* therefore represent hotspots of pelagic denitrification, but the quantitative importance as a sink for bioavailable nitrogen is strongly dependent on the ambient O<sub>2</sub> level. The importance of carcass associated denitrification could be highly significant in O<sub>2</sub> depleted environments such as Oxygen Minimum Zones (OMZ).

Copepods are the most abundant metazoans in the oceans and they represent a central link between primary producers and higher trophic levels of marine food webs (Verity and Smetacek 1996). Furthermore, their grazing and defecation activity are main factors regulating the amount and quality of organic material exported from the oceanic

surface layers to the mesopelagic and benthic communities (Calbet 2001). Through ingestion, digestion and defecation they physically and biogeochemically transform organic material and concentrate it into dense fast sinking pellets (e.g., Rysgaard et al. 1999; Ploug et al. 2008). Copepods also represent a microbial habitat in themselves, with a surface colonized by ambient microbes and an internal microflora that significantly differs from that in the surrounding water (Hansen and Bech 1996; Grossart et al. 2010; Dziallas et al. 2013); nevertheless, direct studies of the biogeochemical implications remain rare (e.g., Proctor 1997; Tang et al. 2010). Functionally anaerobic microbes have been identified in copepods, and methanogenesis has been associated with grazing pelagic copepods (Marty 1993; DeAngelis and Lee 1994). Circumstantial evidence for anaerobic, microbially

Additional Supporting Information may be found in the online version of this article.

\*Correspondence: rnglud@biology.sdu.dk

This is an open access article under the terms of the Creative Commons Attribution-NonCommercial-NoDerivs License, which permits use and distribution in any medium, provided the original work is properly cited, the use is non-commercial and no modifications or adaptations are made.

driven, nitrogen fixation inside copepods has also been presented (Braun et al. 1999). The internal guts of copepods have been proposed as an acidic microenvironment which could have implications for the functioning of gut-associated microbial communities and represent sites of intensified carbonate dissolution (Harris 1994; Jansen and Wolf-Gladow 2001). Recently, microsensor investigations confirmed anaerobic and acidic conditions inside the guts of large, live *Calanus hyperboreus* and *C. glacialis* (Tang et al. 2011), substantiating the potential of anaerobic microbial processing within the guts of live copepods. This potential is expected to be higher in carcasses of copepods where microbial growth and oxygen consumption appear to be intensified (Tang et al. 2009).

Growing evidence suggests that zooplankton can suffer considerably from non-predatory mortality (Hirst and Kiørboe 2002) and zooplankton carcasses are widely observed in water column and sediment trap samples (Hauray et al. 1995; Elliot and Tang 2011a; Ivory et al. 2014; Tang and Elliott 2014). The observations have been ascribed to parasites, viral infection, injuries, starvation and dynamic environmental conditions (Thor et al. 2008; Bickel et al. 2011; Elliot and Tang 2011b). Globally carcasses are assessed to account for on average 12–60% of the total zooplankton in the marine environments, but at the local scales the percentages can be even higher (Tang and Elliot 2014; Tang et al. 2014; Genin et al. 1995; Terazaki and Wada 1988; Wheeler 1967). For example, a recent study from the Arctic documented that up to 94% of the *Calanus* spp. caught between 300 m and 2000 m water depth actually were dead (Daase et al. 2014).

We therefore hypothesize that decomposing copepod carcasses represent microbial hotspots sustaining anaerobic microbial communities mediating denitrification in an otherwise oxygenated ocean. Here we combined O<sub>2</sub> imaging, <sup>15</sup>N tracer experiments and studies on expression of specific functional genes to deduce the potential of denitrification associated with carcasses of *Calanus finmarchicus*, one of the most abundant and widely distributed copepod species in the Northern hemisphere (Helaouët et al. 2011). Data are discussed in the context of potential sinks for bioavailable nitrogen in the ocean.

## Methods

### Study site, copepod sampling and culture conditions

The study was conducted during July 2011 in the area of Godthåbsfjord, Greenland, situated ~ 250 km south of the polar circle. The fjord extends inwards to the Greenland ice cap, covering ~ 2000 km<sup>2</sup> with a mean water depth of 260 m (Mortensen et al. 2011; Juul-Pedersen et al. 2015). Zooplankton were sampled using a plankton net with a mesh size of 200 µm and a non-filtering 1 L cod end (Tang et al. 2011). Net tows extended from 250 m depth to the surface and upon recovery, the cod end content was diluted with surface water and placed in a dark thermo-box kept at ~ 5°C. The samples were returned to the Greenland Institute of Natural Resources (GINR) in

Nuuk within 2–3 h. Subsequently, subsamples were transferred into ice chilled petri dishes (2–5°C) from which 3–4 mm large females of *Calanus finmarchicus* were sorted. Healthy looking copepods were transferred to 2800 mL polycarbonate bottles containing GF/F filtered seawater with a salinity of 34 and were kept at 5°C. The next day, samples were resorted to ensure that experiments were initiated only with healthy individuals. The copepod stock cultures were fed ad libitum with exponentially growing cryptophyte *Rhodomonas salina* and the water was renewed daily.

The *R. salina* culture was kept in 15 L aerated bags filled with 0.2 µm filtered seawater (temperature 20°C and salinity 34) that was diluted daily. The culture was thereby maintained in the exponential growth phase. L-medium (1 mL L<sup>-1</sup>) (Leibovitz, Sigma-Aldrich) was added every second day while the culture was exposed to 12: 12 h dark-light cycles.

To produce well-defined and relatively similar carcasses for controlled experiments, healthy-looking copepods were selected from the 2800 mL stock cultures for two sets of experiments: (1) For denitrification measurements, the copepods were initially fed with a fresh supply of *R. salina* for 15–20 min before they were killed by quickly dipping them in 0.1 N HCl then rinse copiously with filtered seawater—this is a common procedure for carcass production and leave the internal microbial communities unaffected (King et al. 1991); (2) for O<sub>2</sub> imaging the copepods were fed with a mixture of *R. salina* and O<sub>2</sub>-sensitive beads (see below); afterward, the copepods were quickly killed by dipping them in a solution of Tricaine Methanesulfonate (MS222; 0.5g L<sup>-1</sup>) (Carter et al. 2011).

### Oxygen imaging of carcasses

The O<sub>2</sub>-sensitive beads were made from neutrally buoyant, 2–12 µm (average: 5.0 ± 2.5 (SD) µm) spheres of Polystyrene co-Maleic Anhydride (PS-MA) imbedded with Platinum(II) meso 2,3,4,5,6-pentafluoro phenyl porphyrin (PtTFPP) and the antenna dye Macrolex yellow as described by Borisov et al. (2009). The beads were mixed with *R. salina* to an approximate ratio of 1: 20 and fed to *C. finmarchicus*. Faecal pellets released by the copepods contained < 1% (vol vol<sup>-1</sup>) of the beads. Exposure to acid made the copepod's cuticle opaque and therefore individuals selected for imaging were killed with MS222.

For imaging, the heads of fresh carcasses were fixed to 175 µm thin metal wires using a fast curing cyanoacrylates adhesive (Permabond 102). The free ends of the wires were placed in wax mounted to the bottom of a petri dish so that carcasses were lifted ~ 5 mm off the bottom. The water in the petri dish was chilled using a small cooling spiral connected to a thermostat regulated cooling baths, which maintained the temperature of the well mixed sea water at ~ 7°C during the measurements. The O<sub>2</sub> saturation of the ambient seawater was regulated via a digital gas mixer (SensorSense.nl) using compressed atmospheric air and nitrogen gas. The O<sub>2</sub> level was independently monitored by a pre-calibrated optode patch (see below).

The luminescent lifetime of the O<sub>2</sub>-sensitive beads inside the gut of transparent carcasses was recorded with a fast gateable 12-bit Charged Coupled Device camera (SensiCam, PCO) through a 590 nm longpass filter (UQGoptics) (Holst et al. 1998; Frederiksen and Glud 2006). The camera was mounted on a stereomicroscope (Stemi 2000C, Zeiss). Excitation light was delivered by one high power deep blue LED (Osilon4 PowerStar, Osram) equipped with a 470 nm short pass filter (UQGoptics). The operation of camera and LED's were synchronized via a custom made PC-controlled trigger-box and the software Look@Molli (Holst and Grunwald 2001).

The O<sub>2</sub>-sensitive beads were calibrated in artificial seawater (1% vol vol<sup>-1</sup>) using a modified Stern–Volmer equation (Glud et al. 1996). Calibration included five different O<sub>2</sub> levels. Test against beads sitting at the surface of faecal pellets that were microbial inactivated by HgCl<sub>2</sub> addition (0.02 mL saturated solution to mL<sup>-1</sup>) showed identical calibration curves to that of free beads. The established calibration curves were used to calibrate the luminescent lifetime images of the beads inside the transparent carcasses. Carcasses were stepwise exposed to five different O<sub>2</sub> levels from 0% to 100% air saturation. At each O<sub>2</sub> level, a series of 60 images were recorded within ~15 min to confirm quasi steady-state O<sub>2</sub> conditions inside the carcasses. In three instances images were recorded continuously for 3 h at 100% air saturation in the ambient water.

### Incubation of copepod carcasses

To quantify O<sub>2</sub> consumption and denitrification rates associated with *C. finmarchicus* carcasses, a series of incubation with gastight 6–12 mL large vials (Exetainers, Labco) was established. The inner bottom of each vial was affixed with a custom made, O<sub>2</sub>-sensitive fluorescent patch consisting of an O<sub>2</sub> impermeable mylar foil coated with a 5 μm thin coating of PtTFPP in a polystyrene matrix and an upper 100 μm thick layer of black silicone (Wacker N189). The pre-calibrated patches were interrogated from the outside using a commercially available Fibox 3 instrument (PreSens). The O<sub>2</sub> concentration within the individual vials was measured at the beginning and at the end of the incubations. In several selected vials the O<sub>2</sub> concentration was monitored every few hours to confirm a linear decline during incubations that lasted up to 80 h. The vials were filled with 100% air-saturated GF/F filtered seawater (salinity 34) amended with <sup>15</sup>NO<sub>3</sub><sup>-</sup> to a final concentration of 25.0 μmol L<sup>-1</sup>. This provided a total NO<sub>3</sub><sup>-</sup> concentration of 30.0 ± 0.4 (SD) μmol L<sup>-1</sup> in the vials. Incubations were initiated by adding 2–6 freshly produced carcasses to each of the vials. The sealed vials were mounted on a rotating plankton wheel and the speed was adjusted to ensure that carcasses were constantly sinking during the incubations. The incubations were done at 7°C. A total of 28 vials with a total of 109 carcasses were set up, plus three vials without carcasses for control. Vials were gradually sacrificed over time by adding 200 μL saturated

ZnCl<sub>2</sub> to terminate the incubation. The <sup>14</sup>NO<sub>3</sub><sup>-</sup>/<sup>15</sup>NO<sub>3</sub><sup>-</sup> ratio remained constant during the respective incubations.

The accumulated concentrations of <sup>29</sup>N<sub>2</sub> and <sup>30</sup>N<sub>2</sub> of the fixed vials were determined by a gas autosampler in line with a 600°C copper furnace and a 20–22 Isotope Ratio Mass Spectrometer, (Sercon Limited, Crewe) as described by Risgaard-Petersen and Rysgaard (1995). The total denitrification rate in the respective vials was calculated according to the standing isotope-pairing procedure (Nielsen 1992) as applied to homogeneous slurries (Rysgaard and Glud 2004). The concentration of NO<sub>3</sub><sup>-</sup> (+ NO<sub>2</sub><sup>-</sup>) was determined according to Braman and Hendrix (1989).

### Microbiological analysis

To characterize the microbial communities associated with carcasses exposed to conditions similar to those of the <sup>15</sup>N-incubations, a parallel series of 12 vials was established. Initially these vials also contained <sup>15</sup>NO<sub>3</sub><sup>-</sup> amended water with 100% O<sub>2</sub> air-saturation as above. Five carcasses from vials of the parallel series were collected after 0 h, 24 h, 72 h, and 144 h of incubation and were immediately frozen at -80°C. For comparison, the water for incubations, and live, freshly fed copepods from the stock culture were also sampled and frozen in parallel.

To study the expression of specific genes, RNA was extracted from the frozen samples. The genes for which transcripts were targeted included: genes for haem and copper containing nitrite reductase (*nirS* and *nirK*, respectively) involved in denitrification, the gene for methyl co-enzyme-M reductase (*mcrA*) of methanogens and the gene for a methane monooxygenase subunit (*pmoA*) of methanotrophs. For extraction we used chloroform-phenol-isoamyl alcohol and zirconium beads following the protocol of Nercessian et al. (2005), except that we applied 240 mmol L<sup>-1</sup> potassium phosphate buffer. The DNA-RNA-pellet was dissolved in 35 μL, RNase-free water and stored at -80°C. DNA was digested twice with Turbo-DNA free kit (Ambion) following the manufacturer's instructions, except that 2.5 μL of the reaction buffer were used instead of 2 μL. Successful removal of DNA was checked by PCR using the universal primer pair 341f/907r. Subsequently approximately 100 ng of total RNA was used for cDNA synthesis via the Array Script kit (Ambion). The reaction mixtures for PCR amplifications contained 5–20 ng μL<sup>-1</sup> cDNA, 0.4–0.8 pmol μL<sup>-1</sup> of the applied primer pair in a total volume of 50 μL. Details on the respective amplification procedures and conditions are presented in Table 1 of the Supporting Information.

The diversity of the active microbial communities sampled was assessed by Denaturing Gradient Gel Electrophoresis (DGGE) (Rösel et al. 2012) using the PhorU system (Ingenuity), but with different denaturing gradients (see Table 1 of the Supporting Information for details). All gels were stained with SybrGold. The most prominent DGGE bands of the universal primer set and of *nirS* were excised and resolved in 20 μL

tris-ethylene-diamine-tetra-acetic acid (Tris-EDTA, pH 8) buffer for sequencing. The bands were re-amplified using the appropriate primers (Table 1; Supporting Information). PCR products were purified by 1:1 addition of a precipitation solution (20% polyethyleneglycol 8000 and 2.5 mol L<sup>-1</sup> NaCl in distilled water). PCR products were incubated for 20 min, and thereafter centrifuged (at 17,000 × g). The pellets were washed with 100 μL 70% ethanol. Sequencing was performed on an ABI Sequencer 3130 (Applied Biosystems) following the manufacturer's instructions. DGGE bands were sequenced to confirm the PCR products. Analysis of similarities using the software Primer6 was applied to test statistically whether *nirS* gene sequences obtained from live and dead *C. finmarchicus* were significantly different.

#### Abundance of live and dead copepods in Godthåbsfjord

During June 2010, zooplankton was collected at three stations in Godthåbsfjord from the RV "Dana." Samples were collected in 30 m, 50 m, or 100 m depth intervals down to maximum depth of 300 m, using open-close nets (45 μm mesh; 0.125 m<sup>2</sup> mouth diameter) with non-filtering cod ends. The nets were towed through at a very low speed (< 0.5 m s<sup>-1</sup>) and the cod-ends were emptied without rinsing. The total volume of each cod-end sample was measured, and a subsample representing 10–21% of the total was removed for counting copepod carcasses (copepodite and adult stages) under a dissecting microscope on board. Carcasses were identified based on visible tissue loss and decomposition, lack of vital signs (e.g., heart beat or gut peristalsis) and lack of response to external stimulus. Carapaces with no trace of internal tissues were not included. Afterward the subsamples were preserved in Lugol's solution for enumeration of total copepods (live plus dead). Here we report the combined abundance of the three dominant *Calanus* species: *C. finmarchicus*, *C. hyperboreus*, and *C. glacialis*.

## Results

### Oxygen distribution in food-pellets inside *C. finmarchicus* carcasses

The surface of food-pellets within the guts of carcasses exhibited strong but variable O<sub>2</sub> depletion (Fig. 1). Pellets in the cephalosome exhibited stronger O<sub>2</sub> depletion than pellets in the metasome (Fig. 1A,B), but even at 100% air saturation (303 μmol L<sup>-1</sup>) in the ambient water some pellet areas were anoxic. The extent of anoxia increased with decreasing ambient O<sub>2</sub> levels (Fig. 1D). For instance, the average O<sub>2</sub> concentration at the pellet surfaces in the cephalosome and metasome decreased from 90 and 8 μmol L<sup>-1</sup> at 100% air saturation in the ambient water to 40 and 3 μmol L<sup>-1</sup> at 50% air saturation in the ambient water, respectively (Fig. 1D). Three carcasses were investigated and all exhibited the same pattern; data extrapolation indicated that the entire pellet surface would become anoxic at around 15–20% ambient air saturation (45–60 μmol L<sup>-1</sup>) (Fig. 1D). Unfortunately, we did not conduct any long term measurements, but the mean O<sub>2</sub> concentration

at the pellets surface remained constant for at least 3 h at stable experimental conditions. The applied approach only resolves the O<sub>2</sub> availability at the surface of the pellets and the center of the pellets presumably held significantly lower O<sub>2</sub> levels than the pellet surface. The method was therefore only semi-quantitative, but it clearly showed that the interior of *C. finmarchicus* carcasses was strongly O<sub>2</sub> depleted and that even at 100% ambient air saturation, microzones of complete anoxia occurred in the gut.

### Oxygen consumption and denitrification in

#### *C. finmarchicus* carcasses

The O<sub>2</sub> concentration in rotating glass vials containing 2–6 carcasses declined by 0.5–2.0 μM h<sup>-1</sup> during the 7–80 h long incubations, while concentrations in parallel controls containing only sea-water remained constant (not shown). O<sub>2</sub> depletion per carcass was approximated linearly and the average rate equalled 0.41 ± 0.08 (SD) μmol d<sup>-1</sup> (Fig. 2A). The O<sub>2</sub> consumption rate integrates the activity of bacteria associated with the carcasses and that of free living bacteria capitalizing on the DOC that potentially was released.

The integrated denitrification associated with suspended carcasses increased as the O<sub>2</sub> concentration measured at the end of the incubations declined (Fig. 2B). As expected, there was an extensive variation in the measured denitrification rate between parallel vials. This is ascribed to differences in size, age, physiological condition, gut content and potentially the internal microbial communities of the individual copepods before they were killed. The isotope pairing technique enabled us to assess the relative importance of NO<sub>3</sub><sup>-</sup> sources sustaining the process of denitrification, and on average nitrification provided 34% ± 17% (SD, *n* = 28) of the NO<sub>3</sub><sup>-</sup> fuelling the integrated denitrification. There was no clear relation between the relative importance of nitrification in sustaining denitrification and the ambient O<sub>2</sub> concentration in the vials, both measured at the end of the incubations (data not shown). It is, however, important to realize that the integrated denitrification and the relative importance of coupled denitrification were measured on the background of a linearly declining O<sub>2</sub> concentration in the vials and therefore, it provided only an integrated signal. In reality, the instantaneous denitrification (and potentially coupled nitrification) is expected to respond nonlinearly to the decline in O<sub>2</sub> concentration. To derive the instantaneous denitrification rate within the carcasses as a function of the ambient O<sub>2</sub> concentration the following relationship for the measured, integrated denitrification rate, *D<sub>I</sub>*, was established, assuming an exponential decay of activity with increasing oxygen as observed by Dalsgaard et al. (2014):

$$D_I = \int_0^t D_m e^{-K(\alpha t + \beta)} dt \quad (1)$$

Here, *t* is the incubation time, *D<sub>m</sub>* the maximum denitrification rate, *K* is a decay constant expressing the inhibition of denitrification by the ambient O<sub>2</sub> level, *α* is the rate of O<sub>2</sub>

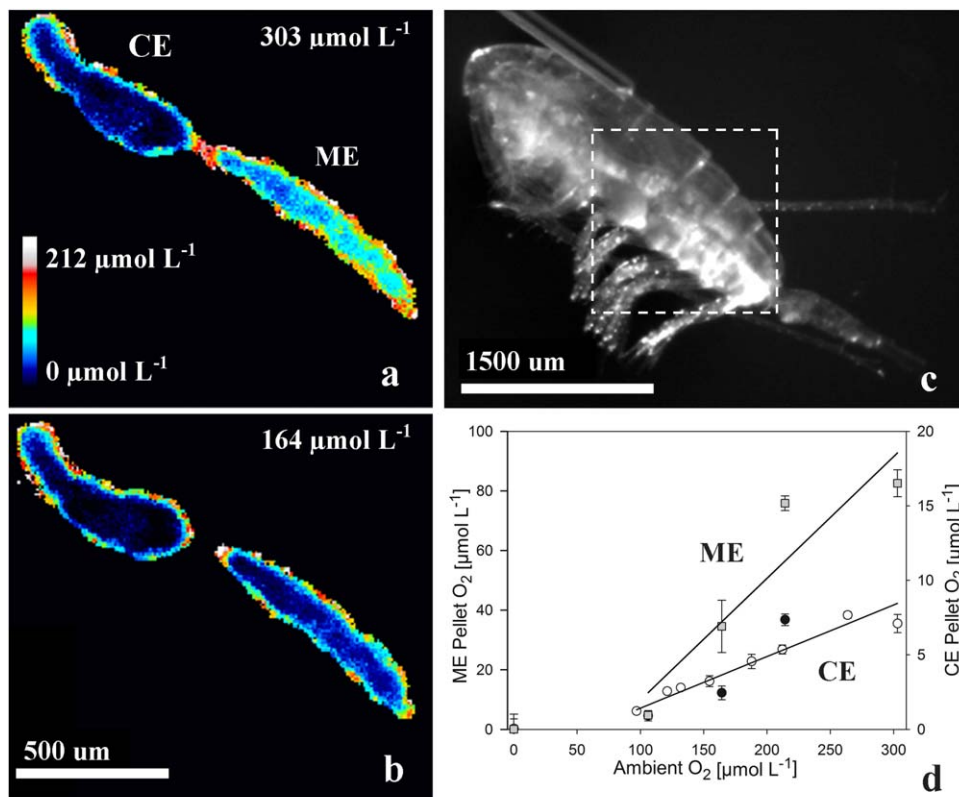


**Fig. 1.** Oxygen images of the gut interior in a carcass of *C. finmarchicus* at ambient O<sub>2</sub> concentration of 303 μmol L<sup>-1</sup> (a) and 164 μmol L<sup>-1</sup> (b). Oxygen levels were more depleted in the anterior cephalosome (CE) as compared to posterior metasoma (ME). The carcasses were fixed on small metal wires glued to the head region (c) and positioned ~ 5 mm off the bottom of a well-mixed water bath. The square framed by broken lines in (c) represent the area of O<sub>2</sub> images depicted in (a, b). The average O<sub>2</sub> concentration at the pellet surface decreased with the O<sub>2</sub> availability in the ambient water. Three carcasses were investigated, but only one individual had a pellet in the cephalosome (d), different symbols represent different carcasses. Error bars indicate the SE.

decline and  $\beta$  is the initial O<sub>2</sub> concentration in the respective vials. Assuming a stoichiometric ratio between carbon oxidation by O<sub>2</sub> and that by NO<sub>3</sub><sup>-</sup> of 1: 0.8 (Berner 1971) and using the average O<sub>2</sub> consumption rate (0.41 μmol carcass<sup>-1</sup> d<sup>-1</sup>), the maximum denitrification ( $D_m$ ) is estimated to be 0.32 μmol N carcass<sup>-1</sup> d<sup>-1</sup>. The values of  $D_1$ ,  $\alpha$  and  $\beta$  are directly measured in each of the respective incubations making it possible to determine  $K$  by solving Eq. 1:

$$D_1 = (-D_m/\alpha K)e^{-K\beta}(e^{K\alpha t} + 1) \tag{2}$$

Using a non-linear least squares fit procedure including all the measured values,  $K$  was determined to be 0.108 μM<sup>-1</sup>. The instantaneous denitrification rate ( $D$ ; μmol N carcass<sup>-1</sup> d<sup>-1</sup>) as a function of the ambient O<sub>2</sub> concentration ( $C$ ; μmol L<sup>-1</sup>) at the given experimental conditions (7°C and salinity 34) can then be described by:

$$D = 0.32e^{-0.108C} \tag{3}$$

The re-modelled values of integrated denitrification using the determined  $K$  matched the measured data points relatively well and paired values distributed evenly around  $X = Y$

(Fig. 2C). We cannot fully exclude any contribution of anammox to the overall N<sub>2</sub> production. However, such potential contributions must have been minor as we observed no significant skewness in the expected ratio between <sup>29</sup>N<sub>2</sub> and <sup>30</sup>N<sub>2</sub> production assuming their production solely was related to denitrification (Risgaard-Petersen et al. 2003).

**Microbial communities and gene expression in carcasses of *C. finmarchicus***

Whereas microbial communities in the ambient water did not express any of the tested genes involved in denitrification (*nirK*, *nirS*), the *nirS* gene was expressed in all 12 samples of *C. finmarchicus* carcasses and in 5 of the 12 samples of live *C. finmarchicus* (Table 1). The samples did not resolve any temporal development in the gene expression. The *nirK* gene was not expressed in any sample. Likewise, none of the tested genes involved in methane turn-over (*mcrA*, *pmoA*) were expressed in the few carcasses and live copepods examined (Table 1).

Diversity of the dominant and sequenced DGGE bands obtained after PCR of partial 16S rDNA was relatively low. In both dead and live *C. finmarchicus* samples, *Shewanella* species dominated. Some carcasses revealed bright DGGE

bands of a *Pseudoalteromonas* strain, 2 *Moritella* strains and a gammaproteobacterium (Table 2, Supporting Information). Apart from *Shewanella*, live animals showed bright DGGE

bands of a *Salinibacterium*, a *Chloroflexi*, an *Actinobacterium* and a *Chromobacterium* strain. The most dominant bands in ambient seawater differed from those on carcasses and live copepods (Table 2 Supporting Information).

**Abundance of copepods and carcasses in Godthåbsfjord**

The natural abundance of calanus species (i.e., *finmarchicus*, *hyperboreus* and *C. glacialis*) were determined off shore, at the entrance and in the inner part of Godthåbsfjord during summer 2010 (Fig. 3). Carcasses accounted for 4% of the total *Calanus* abundance in the surface waters at the off shore station to 76% at intermediary depth in the inner part of the fjord. In absolute numbers the amount of carcasses ranged from 4 m<sup>-3</sup> to 95 m<sup>-3</sup> depending on depth and location (Fig. 3). Integrating the values to the deepest sampling depth at the respective stations, the number of carcasses corresponded to 7900 m<sup>-2</sup>, 1800 m<sup>-2</sup>, and 8790 m<sup>-2</sup> at the three stations, respectively.

**Discussion**

Microbial denitrification represents an important sink for bioavailable nitrogen in many marine settings and is generally considered to be an anaerobic process (Robertson and Kuenen 1984; Zumft 1997; Devol 2015). Significant denitrification rates are therefore confined to anoxic water bodies, sediments and melting sea-ice (Rysgaard and Glud 2004; Dalsgaard et al. 2012, 2014; Devol 2015), but anoxic microniches within otherwise oxic environments remain underexplored potential sites for denitrification activity. Sinking phytoplankton aggregates have been identified as potential sites of anoxia (Allredge and Cohen 1987; Ploug et al. 1997) and recent evidence suggests that these microsites could host anaerobic processes of N-transformation, especially in water bodies with reduced content of O<sub>2</sub> (Klawonn et al. 2015; P. Stief et al. pers. comm.) or upon sedimentation (Lehto et al. 2014). Here we document that carcasses of one of the most dominant metazoans in the marine pelagic biome host microbial communities of active denitrifiers.

Expression of *nirS* genes was detectable in all carcasses even at full air-saturation in the ambient water (302 μmol L<sup>-1</sup>) (Table 1) and O<sub>2</sub> imaging confirmed localized anoxia inside the carcasses (Fig. 1). However, replicate incubations exhibited variation of up to 1–2 orders of magnitude in denitrification rates and a carcass-specific denitrification rate of 0.8 nmol N d<sup>-1</sup> at 100% air saturation was encountered in a single incubation (Fig. 2B). But generally average

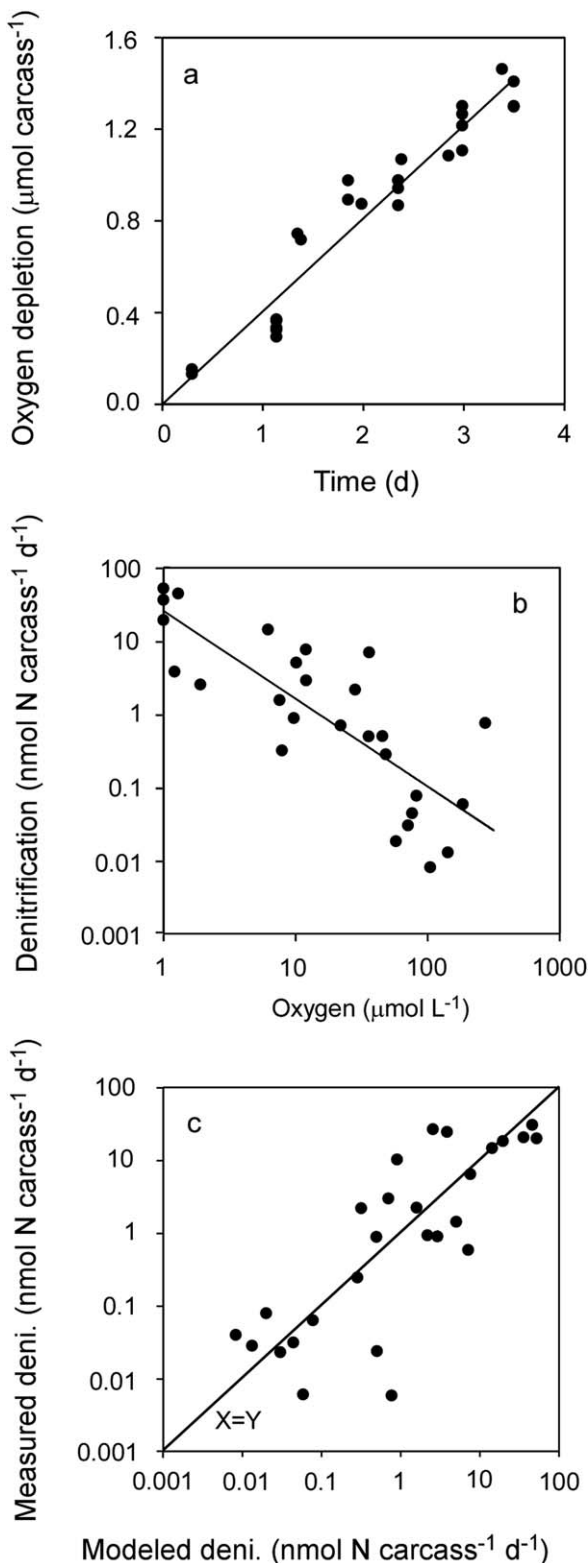


**Fig. 2.** (a) The amount of O<sub>2</sub> consumed per carcass as a function of time. The data are approximated by the best linear fit passing Origin; Y = 0.41 (R<sup>2</sup> = 0.93). (b) The integrated denitrification rate in sinking carcasses depicted as a function of the available O<sub>2</sub> concentration measured at the end of the incubation (closed symbol). The measured data are approximated by a simple power function Y = 25.6 X<sup>-1.2</sup> (R<sup>2</sup> = 0.65). The integrated denitrification rates modelled using Eq. 1 and the most optimal universal inhibition constant K (0.108 μM<sup>-1</sup>) vs. the measured rates are shown in panel c. See text for details in the modelling approach.



**Table 1.** Functional gene analyses in ambient water (W) and on five pooled carcasses (C) or live specimens (L) of *C. finmarchicus*. The time of sampling after the incubation was initiated is indicated in the second column. Boxes without notations means not studied, while; -, + means negative and positive signals, respectively.

| Sample | Time (h) | cDNA (ng $\mu\text{L}^{-1}$ ) | nirK | nirS | mcrA | pmoA |
|--------|----------|-------------------------------|------|------|------|------|
| W      | 2        | 5                             | -    | -    |      |      |
| W      | 2        | 12                            | -    | -    |      |      |
| C      | 0        | 72                            | -    | +    |      |      |
| C      | 24       | 116                           | -    | +    | -    |      |
| C      | 24       | 95                            | -    | +    |      |      |
| C      | 24       | 4                             | -    | +    |      |      |
| C      | 72       | 121                           | -    | +    | -    |      |
| C      | 72       | 81                            | -    | +    | -    |      |
| C      | 72       | 40                            | -    | +    |      |      |
| C      | 72       | 145                           | -    | +    | -    | -    |
| C      | 72       | 92                            | -    | +    | -    | -    |
| C      | 72       | 57                            | -    | +    |      |      |
| C      | 144      | 69                            | -    | +    |      |      |
| C      | 144      | 44                            | -    | +    |      |      |
| L      | 0        | 5                             | -    | -    |      |      |
| L      | 24       | 34                            | -    | +    |      |      |
| L      | 24       | 10                            | -    | -    |      |      |
| L      | 72       | 12                            | -    | -    |      |      |
| L      | 72       | 26                            | -    | +    |      |      |
| L      | 72       | 9                             | -    | -    |      |      |
| L      | 72       | 273                           | -    | -    |      |      |
| L      | 72       | 136                           | -    | -    | -    |      |
| L      | 144      | 48                            | -    | +    | -    | -    |
| L      | 144      | 40                            | -    | -    | -    |      |
| L      | 144      | 8                             | -    | +    |      |      |
| L      | 144      | 45                            | -    | +    | -    | -    |

denitrification rates at high ambient O<sub>2</sub> levels were low (~ 0.01 nmol N carcass<sup>-1</sup> d<sup>-1</sup>; Fig. 2). A high degree of variation among replicates was expected as the history, size, food content and associated microbial communities likely varied among the carcasses. On average, carcass specific denitrification rates exceeding 1 nmol N d<sup>-1</sup> were reached when the ambient O<sub>2</sub> levels declined below ~ 55  $\mu\text{mol L}^{-1}$  as given by Eq. 3. This threshold corresponds to the ambient O<sub>2</sub> level when complete anoxia was observed in the carcass guts (Fig. 1D).

In parallel to our carcass investigation, we conducted some investigations on live *C. finmarchicus*. Oxygen imaging confirmed previous invasive mirosensor measurements (Tang et al. 2011) and documented anoxia in pellets passing through the guts of immobilized but actively feeding copepods (data not shown). Despite the occasional expression of *nirS* genes in live specimens, we were not able to detect any significant denitrification activity by <sup>15</sup>NO<sub>3</sub><sup>-</sup> amendments in the 15 incubations that we conducted. However, only six of these incubations went below O<sub>2</sub> levels of 50  $\mu\text{mol L}^{-1}$  and we cannot exclude that live *C. finmarchicus* can facilitate significant internal denitrification at lower O<sub>2</sub> levels or at different environmental settings. Interestingly, analysis of similarities (ANOSIM) showed that *nirS* sequences on carcasses were different from those on live copepods (Supporting Information Fig. 1). This suggests that the microenvironment of freshly produced carcasses selects for specific subpopulation of denitrifiers.

We were not able to detect any expression of *mcrA* (for methanogenesis) or *pmoA* (for methane oxidation) gene in either carcasses or live specimens. Local elevated methane concentrations in marine waters have previously been linked to the presence of zooplankton (Marty 1993; DeAngelis and Lee 1994), but apparently no methane turn-over was associated to the population of *C. finmarchicus* investigated in Godthåbsfjord.

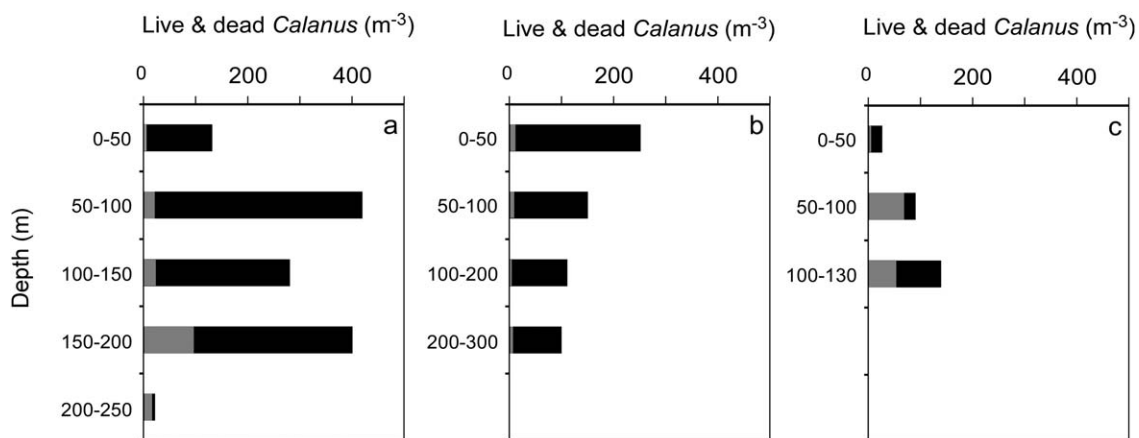


**Fig. 3.** Abundance of live (black) and dead (grey) *Calanus* species (*C. finmarchicus*, *C. hyperboreus* and *C. glacialis*) as collected at three stations in Godthåbsfjord: (a) off shore station (63°58.67N, 52°23.47W), (b) entrance (64°23.91N, 51°33.59W), (c) inner fjord (64°26.10N, 50°39.02W).

The amount of carcasses of larger *Calanus* species in Godthåbsfjord ranged from  $4 \text{ m}^{-3}$  to  $95 \text{ m}^{-3}$  specimens, integrated to the deepest sampling depths this was equivalent to an average of  $6200 \pm 3800$  carcasses per  $\text{m}^2$ . These values are difficult to extrapolate in time and space, but provide an estimate for carcass abundances in the study area during summer. The value falls within the range of reported copepod carcass abundances in the world's oceans (Tang and Elliott 2014). Given that the pelagic zone of Godthåbsfjord is generally well oxygenated and that the bottom water in isolated basins reach values below  $200 \mu\text{mol O}_2 \text{ L}^{-1}$  only during seasonal stratification (H. L. Sørensen et al. pers. comm.), carcass associated denitrification at the measured densities would only amount to  $\sim 60 \text{ nmol N m}^{-2} \text{ d}^{-1}$ , or less than a few per mille of the benthic denitrification rate of  $\sim 125 \mu\text{mol N m}^{-2} \text{ d}^{-1}$  in the study area (H. L. Sørensen et al. pers. comm.). Nevertheless, considering the strong dependence on ambient oxygen levels (Fig. 2), the potential importance of carcass associated denitrification would be much higher in regions with lower ambient oxygen levels.

The volume specific rates of denitrification in oxygen minimum zones (OMZ's) typically range from  $2 \text{ nmol N L}^{-1} \text{ d}^{-1}$  to  $50 \text{ nmol N L}^{-1} \text{ d}^{-1}$  (e.g., Ward et al. 2009; Dalsgaard et al. 2012; De Brabandere et al. 2014) and are generally confined to water with ambient  $\text{O}_2$  levels below  $2 \mu\text{mol L}^{-1}$  (Dalsgaard et al. 2014; De Brabandere et al. 2014). At this oxygen level, this range of denitrification rates could be attained by carcass associated denitrification at carcass abundances of  $6\text{--}150 \text{ m}^{-3}$ , as predicted by Eq. 3. Such abundances of copepod carcasses are not uncommon in many marine settings (Tang and Elliot 2014). As an example, the central Arabian sea with an anoxic core (i.e.,  $< 2 \mu\text{mol O}_2 \text{ L}^{-1}$ ) from 100 m to  $> 1000$  m contained an average abundance of copepod carcasses in the order of  $50 \text{ m}^3$  (Böttger-Schnack 1996). Assuming that our findings in Godthåbsfjord could be extrapolated to the conditions in the central Arabian Sea, the average carcass associated denitrification rate would be a significant  $16 \text{ nmol N L}^{-1} \text{ d}^{-1}$ .

Equation 3 predicts a carcass specific denitrification rate of  $260 \text{ nmol N d}^{-1}$  at  $2 \mu\text{mol O}_2 \text{ L}^{-1}$ ,  $110 \text{ nmol N d}^{-1}$  at  $10 \mu\text{mol O}_2 \text{ L}^{-1}$  and  $22 \text{ nmol N d}^{-1}$  at  $25 \mu\text{mol O}_2 \text{ L}^{-1}$ . The presence of copepod carcasses thereby markedly increases the volume of water in OMZ regions that could act as a sink for bioavailable nitrogen. For instance, the oceanic volume of the five major global oceans having  $\text{O}_2$  levels  $< 5 \mu\text{mol L}^{-1}$  is assessed to be in the order of  $0.46 \times 10^5 \text{ m}^3$ , while the volume having  $\text{O}_2$  levels  $< 55 \mu\text{mol L}^{-1}$  is estimated to be 45 times larger (Karstensen et al. 2008). The presence of even moderate abundances of sinking carcasses could therefore substantially add to the presently assessed denitrification rates associated with OMZ's. The abundance of copepod carcasses during late summer in the NW Pacific ( $44^\circ\text{N}, 155^\circ\text{E}$ ) has previously been quantified at  $15\text{--}200 \text{ m}^{-3}$  at depth  $100\text{--}3500$  m, with mean values of  $65 \text{ m}^{-3}$  in the core of the OMZ (Yamaguchi et al. 2002). Concurrent  $\text{O}_2$  measurements showed oxygen decreased to a minimum of  $15\text{--}20 \mu\text{mol O}_2 \text{ L}^{-1}$  in the OMZ core at  $500\text{--}800$  m, then gradually rose to  $150 \mu\text{mol}$

$\text{O}_2 \text{ L}^{-1}$  at  $3500$  m depth (Yamaguchi et al. 2002). Using Eq. 3 we estimated a maximum carcass associated denitrification rate of  $\sim 4 \text{ nmol N L}^{-1} \text{ d}^{-1}$  in the OMZ core and a depth integrated rate of  $\sim 2000 \mu\text{mol N m}^{-2} \text{ d}^{-1}$  in this region, which is comparable to many benthic denitrification rates measured in costal sediments (Devol 2015). The NW Pacific is currently not expected to host any pelagic denitrification, but our calculations suggest that carcass associated denitrification could be a significant but hitherto overlooked nitrogen sink in this region.

While the experimental conditions (temperature  $7^\circ\text{C}$ , nitrate levels of  $30 \mu\text{mol L}^{-1}$ ) would be typical for many non-photocostal, shelf and even deep-sea environments, extrapolation of our findings to the natural environment should only be done with caution. Marine copepods can differ significantly in their biology, their feeding behavior and the size from the specie we used (*C. finmarchicus*). For the experiments we produced carcasses from healthy and well fed animals, which will not necessarily reflect conditions for all carcasses in the natural environment. Nonetheless, using complementary approach integrating a range of different techniques, we showed that copepod carcasses hosted an anoxic interior with an active microbial community of denitrifiers. Considering the high abundances of copepods and the prevalence of their carcasses globally, their associated denitrification activities demand further investigation and potentially a revision of the estimated pelagic removal rates of bioavailable nitrogen.

## References

- Allredge, A. L., and Y. Cohen. 1987. Can microscale chemical patches persist in the sea? Microelectrode study of marine snow and fecal pellets. *Science* **235**: 689–691. doi:10.1126/science.235.4789.689
- Berner, R. A. 1971. Principles of chemical sedimentology, 240 p. McGraw-Hill.
- Bickel, S. L., J. D. M. Hammond, and K. Tang. 2011. Boat-generated turbulence as a potential source of mortality among copepods. *J. Exp. Mar. Biol. Ecol.* **410**: 105–109. doi:10.1016/j.jembe.2011.02.038
- Borisov, S. M., T. Mayr, G. Mistlberger, K. Waich, K. Koren, P. Chojnacki, and I. Klimant. 2009. Precipitation as a simple and versatile method for preparation of optical nanochemosensors. *Talanta* **79**: 1322–1330. doi:10.1016/j.talanta.2009.05.041
- Böttger-Schnack, R. 1996. Vertical structure of small metazoan plankton, especially non-calaniid copepods. I. Deep Arabian Sea. *J. Plankton Res.* **18**: 1073–1101. doi:10.1093/plankt/18.7.1073
- Braman, R. S., and S. A. Hendrix. 1989. Nanogram nitrite and nitrate determination in environmental and biological materials by vanadium (III) reduction with chemiluminescence detection. *Anal. Chem.* **61**: 2715–2718. doi:10.1021/ac00199a007

- Braun, S. T., L. M. Proctor, S. Zani, M. T. Mellon, and J. P. Zehr. 1999. Molecular evidence for zooplankton-associated nitrogen-fixing anaerobes based on amplification of the *nifH* gene. *FEMS Microb. Ecol.* **28**: 273–279. doi:10.1111/j.1574-6941.1999.tb00582.x
- Calbet, A. 2001. Mesozooplankton grazing impact on primary production: A global comparative analysis in marine ecosystems. *Limnol. Oceanogr.* **46**: 1824–1830. doi:10.4319/lo.2001.46.7.1824
- Carter, K., C. M. Woodley, and R. S. Brown. 2011. A review of tricaine methanesulfonate for anesthesia of fish. *Rev. Fish. Biol. Fish.* **21**: 51–59. doi:10.1007/s11160-010-9188-0
- Daase, M., Ø. Varpe, and S. Falk-Petersen. 2014. Non-consumptive mortality in copepods: Occurrence of *Calanus* spp. Carcasses in the Arctic Ocean during winter. *J. Plankton Res.* **36**:129–144. doi:10.1093/plankt/fbt079
- Dalsgaard, T., B. Thamdrup, L. Farias, and N. P. Revsbech. 2012. Anammox and denitrification in the oxygen minimum zone of the eastern South Pacific. *Limnol. Oceanogr.* **57**: 1331–1346. doi:10.4319/lo.2012.57.5.1331
- Dalsgaard, T., and others. 2014. Oxygen nanomolar levels reversibly suppress process rates and gene expression in anammox and denitrification in the oxygen minimum zone. *Mbio* **5**: e01966–14. doi:10.1128/mBio.01966-14
- DeAngelis, M. A., and C. Lee. 1994. Methane production during zooplankton grazing on marine phytoplankton. *Limnol. Oceanogr.* **39**: 1298–1308.
- De Brabandere, L., D. E. Canfield, T. Dalsgaard, G. E. Friederich, N. P. Revsbech, O. Ulloa, and B. Thamdrup. 2014. Vertical partitioning of nitrogen-loss processes across the oxic-anoxic interface of an oceanic oxygen minimum zone. *Environ. Microb.* **16**: 3041–3054. doi:10.1111/1462-2920.12255
- Devol, A. H. 2015. Denitrification, Anammox, and N<sub>2</sub> production in marine sediments. In C. A. Carlson, and S. J. Giovannoni [eds] *Annual Review of Marine Science*, vol 7. Annual Reviews Publishers. doi:10.1146/annurev-marine-010213-135040
- Dziallas, C., H. P. Grossart, K. W. Tang, and T. G. Nielsen. 2013. Distinct communities of free-living and copepod associated microorganisms along a salinity gradient in Godthåbsfjord, West Greenland. *Arct. Antarct. Alp. Res.* **45**: 471–480. doi:10.1657/1938-4246.45.4.471
- Elliot, D. T., and K. W. Tang. 2011a. Spatial and temporal distribution of live and dead copepods in the lower Chesapeake Bay (Virginia, USA). *Estuar. Coast.* **34**: 1039–1048. doi:10.1007/s12237-011-9380-z
- Elliot, D. T., and K. W. Tang. 2011b. Influence of carcass abundance on estimates of mortality and assessment of population dynamics in *Acartia tonsa*. *Mar. Ecol. Prog. Ser.* **427**: 1–12. doi:10.3354/meps09063
- Frederiksen, M. S., and R. N. Glud. 2006. Oxygen dynamics in the rhizosphere of *Zostera marina*: A two-dimensional planar optode study. *Limnol. Oceanogr.* **51**: 1072–1083. doi:10.4319/lo.2006.51.2.1072
- Genin, A., G. Gal, and L. Hauray. 1995. Copepod carcasses in the Ocean. II. Nera Coral Reefs. *Mar. Ecol. Prog. Ser.* **123**: 65–71. doi:10.3354/meps123065
- Glud, R. N., N. B. Ramsing, J. K. Gundersen, and I. Klimant. 1996. Planar optodes, a new tool for fine scale measurements of two dimensional O<sub>2</sub> distribution in benthic communities. *Mar. Ecol. Prog. Ser.* **140**: 217–226. doi:10.3354/meps140217
- Grossart, H. P., C. Dziallas, F. Leunert, and K. Tang. 2010. Bacteria dispersal by hitchhiking on zooplankton. *Proc. Natl. Acad. Sci.* **107**: 11959–11964. doi:10.1073/pnas.1000668107
- Hansen, B., and G. Bech. 1996. Bacteria associated with a marine planktonic copepod culture. I. Bacterial genera in seawater, body surface, intestines and fecal pellets and succession during fecal pellet degradation. *J. Plankton Res.* **18**: 257–273. doi:10.1093/plankt/18.2.257
- Harris, R. P. 1994. Zooplankton grazing on the coccolithophore *Emiliania huxleyi* and its role in inorganic carbon flux. *Mar. Biol.* **119**: 431–439. doi:10.1007/BF00347540
- Hauray, L., C. Frey, G. Gal, A. Hobday, and A. Genin. 1995. Copepod carcasses in the Ocean. I. Over seamounts. *Mar. Ecol. Prog. Ser.* **123**: 57–63. doi:10.3354/meps123057
- Helaouët, P., G. Beugrand, and P. C. Reid. 2011. Macrophysiology of *Calanus finmarchicus* in the North Atlantic Ocean. *Prog. Oceanogr.* **91**: 217–228. doi:10.1016/j.pocean.2010.11.003
- Hirst, A. G., and T. Kiørboe. 2002. Mortality of marine planktonic copepods: Global rates and patterns. *Mar. Ecol. Prog. Ser.* **230**: 195–209. doi:10.3354/meps230195
- Holst, G., and B. Grunwald. 2001. Luminescence lifetime imaging with transparent oxygen optodes. *Sens. Actuators B-Chem.* **74**: 78–90. doi:10.1016/S0925-4005(00)00715-2
- Holst, G., O. Kohls, I. Klimant, B. König, M. Kuhl, and T. Richter. 1998. A modular luminescence lifetime imaging system for mapping oxygen distribution in biological samples. *Sens. Actuators B-Chem.* **51**: 163–170. doi:10.1016/S0925-4005(98)00232-9
- Ivory, J. A., K. W. Tang, and K. Takahashi. 2014. Use of neutral red in short-term sediment traps to distinguish between zooplankton swimmers and carcasses. *Mar. Ecol. Prog. Ser.* **505**: 107–117. doi:10.3354/meps/10775
- Jansen, H., and D. A. Wolf-Gladrow. 2001. Carbonate dissolution in copepod guts: A numerical model. *Mar. Ecol. Prog. Ser.* **221**: 199–207. doi:10.3354/meps221199
- Juul-Pedersen, T., K. E. Arendt, J. Mortensen, M. E. Blicher, D. H. Søgaard, and S. Rysgaard. 2015. Seasonal and inter-annual phytoplankton production in a sub-Arctic tide-water outlet glacier fjord, SW Greenland. *Mar. Ecol. Prog. Ser.* **524**: 27–38. doi:10.3354/meps11174
- Karstensen, J., L. Stamma, and M. Visbeck. 2008. Oxygen minimum zones in the eastern tropical Atlantic and Pacific Oceans. *Prog. Oceanogr.* **77**: 331–350. doi:10.1016/j.pocean.2007.05.009
- King, C., R. Sanders, E. Shotts, Jr., and K. Porter. 1991. Differential survival of bacteria ingested by zooplankton

- from a stratified eutrophic lake. *Limnol. Oceanogr.* **36**: 829–845. doi:10.4319/lo.1991.36.5.0829
- Klawonn, I., S. Bonaglia, V. Brüchert, and H. Ploug. 2015. Aerobic and anaerobic nitrogen transformation processes in N<sub>2</sub>-fixing cyanobacterial aggregates. *ISME J.* **9**: 1456–1466. doi:10.1038/ismej.2014.232
- Lehto, N., R. N. Glud, G. a Nordi, H. Zang, and W. Davison. 2014. Anoxic microniches in marine sediments induced by aggregate settlement: Biogeochemical dynamics and implications. *Biogeochemistry* **119**: 307–327. doi:10.1007/s10533-014-9967-0
- Marty, D. G. 1993. Methanogenic bacteria in seawater. *Limnol. Oceanogr.* **38**: 452–456. doi:10.4319/lo.1993.38.2.0452
- Mortensen, J., K. Lennert, J. Bendtsen, and S. Rysgaard. 2011. Heat sources for glacial melt in the sub-Arctic fjord (Godthåbsfjord) in contact with the Greenland Ice sheet. *J. Geophys. Res.* **116**: C01913. doi:10.1029/2010JC006528
- Nercessian, O., E. Noyes, M. G. Kalyuzhnaya, M. E. Lidstrom, and L. Christoserdova. 2005. Bacterial populations active in metabolism of C 1 compounds in the sediment of Lake Washington, a freshwater lake. *Appl. Environ. Microbiol.* **71**: 6885–6899. doi:10.1128/AEM.71.11.6885-6899.2005
- Nielsen, L. P. 1992. Denitrification in sediment determined from nitrogen isotope pairing. *FEMS Microb. Ecol.* **86**: 357–362. doi:10.1016/0378-1097(92)90800-4
- Ploug, H., M. Kuhl, B. BuchholzCleven, and B. B. Jørgensen. 1997. Anoxic aggregates—an ephemeral phenomenon in the pelagic environment. *Aquat. Microb. Ecol.* **13**: 285–294. doi:10.3354/ame013285
- Ploug, H., M. H. Iversen, M. Koski, and E. T. Buitenhuis. 2008. Production, oxygen respiration rates, and sinking velocity of copepod fecal pellets: Direct measurements of ballasting opal and calcite. *Limnol. Oceanogr.* **53**: 469–476. doi:10.4319/lo.2008.53.2.0469
- Proctor, L. M. 1997. Nitrogen-fixing, photosynthetic, anaerobic bacteria associated with pelagic copepods. *Aquat. Microb. Ecol.* **12**: 105–113. doi:10.3354/ame012105
- Risgaard-Petersen, N., and S. Rysgaard. 1995. Nitrate reduction in sediments and water logged soil measured by <sup>15</sup>N techniques, p. 287–295. *In* K. Alef and P. Nannipieri [eds.], *Methods in applied soil and microbiology*. Academic.
- Risgaard-Petersen, N., L. P. Nielsen, S. Rysgaard, T. Dalsgaard, and R. L. Meyer. 2003. Application of the isotope pairing techniques in sediments where anammox and denitrification coexist. *Limnol. Oceanogr.* **1**: 63–73.
- Robertson, L. A., and J. G. Kuenen. 1984. Aerobic denitrification—old wine in new bottles? *Antonie van Leeuwenhoek* **50**: 525–544. doi:10.1007/BF02386224
- Rösel, S., A. Rychła, C. Wurzbacher, and H. P. Grossart. 2012. Effects of pollen leaching and microbial degradation on organic carbon and nutrient availability in lake water. *Aquat. Sci.* **74**: 87–99. doi:10.1007/s00027-011-0198-3
- Rysgaard, S., T. G. Nielsen, and B. Hansen. 1999. Seasonal variation in nutrients, pelagic primary production and grazing in a high-Arctic coastal marine ecosystem, Young Sound, Northeast Greenland. *Mar. Ecol. Prog. Ser.* **179**: 13–25. doi:10.3354/meps179013
- Rysgaard, S., and R. N. Glud. 2004. Anaerobic N<sub>2</sub> production in Arctic sea-ice. *Limnol. Oceanogr.* **49**: 86–94. doi:10.4319/lo.2004.49.1.0086
- Tang, K., S. Bikel, C. Dziallas, and H. P. Grossart. 2009. Microbial activities accompanying decomposition of cladoceran and copepod carcasses under different environmental conditions. *Aquat. Microb. Ecol.* **57**: 89–100. doi:10.3354/ame01331
- Tang, K. W., V. Turk, and H. P. Grossart. 2010. Linkage between crustacean zooplankton and aquatic bacteria. *Aquat. Microb. Ecol.* **61**: 261–277. doi:10.3354/ame01424
- Tang, K. W., R. N. Glud, A. Glud, S. Rysgaard, and T. G. Nielsen. 2011. Copepod guts as biogeochemical hotspots in the sea: Evidence from microelectrode profiling of *Calanus* spp. *Limnol. Oceanogr.* **56**: 666–672. doi:10.4319/lo.2011.56.2.0666
- Tang, K. W., and D. T., Elliott. 2014. Copepod carcasses: Occurrence, fate and ecological importance. p. 255–278. *In* L. Seuront [ed.] *Copepods: Diversity, habitat and behaviour*. Nova Science Publishers.
- Tang, K. W., M. I. Gladyshev, O. P. Dubovskaya, G. Kirillin, and H. P. Grossart. 2014. Zooplankton carcasses and non-predatory mortality in freshwater and inland sea environments. *J. Plankton Res.* **36**: 597–612. doi:10.1093/plankt/fbu014
- Terazaki, M., and M. Wada. 1988. Occurrence of large numbers of carcasses of the large grazing copepod *Calanus cristatus* from the Japan Sea. *Mar. Biol.* **97**: 177–183. doi:10.1007/BF00391300
- Thor, P., T. G. Nielsen, and P. Tiselius. 2008. Mortality rates of epipelagic copepods in the post-spring bloom period in Disko Bay, Western Greenland. *Mar. Ecol. Prog. Ser.* **359**: 151–160. doi:10.3354/meps07376
- Verity, P. G., and V. Smetasek. 1996. Organism life cycles, predation and the structure of marine pelagic ecosystems. *Mar. Ecol. Prog. Ser.* **130**: 277–293. doi:10.3354/meps130277
- Ward, B. B., and others. 2009. Denitrification as dominant nitrogen loss process in the Arabian Sea. *Nature* **461**: 78–U77. doi:10.1038/nature08276
- Wheeler, E. H. 1967. Copepod detritus in the deep sea. *Limnol. Oceanogr.* **12**: 697–701. doi:10.4319/lo.1967.12.4.0697
- Yamaguchi, A., and others. 2002. Community and thropic structures of pelagic copepods down to greater depths in the western subarctic Pacific (West-COSMIC). *Deep-Sea Res.* **49**: 1007–1025. doi:10.1016/S0967-0637(02)00008-0
- Zumft, W. G. 1997. Cell biology and molecular basis of denitrification. *Microbiol. Mol. Biol. Rev.* **61**: 533–616.

#### Acknowledgments

We would like to thank A. Glud for technical support and S. Pinnow for performing the molecular analyses. Dr J. Karstensen for providing

original data of a previously published figure expressing assessed oceanic volumes of different oxygen levels (Karstensen et al. 2008). The study was financially supported by grants from Danish Council for Independent Research (95-306-23437 and 0602-02276B), Villum Foundation (95-306-13881), the Commission for Scientific Research in Greenland (GCRC6507 & 6505), European Research Council through an Advanced Grant (ERC-2010-AdG20100224), the Danish National Research Foundation (DNRF53 to Nordic Center for Earth Evolution), the board of the Danish Centre for Marine Research, DCH (BOFYGO), and by a grant

from the German Science Foundation (DFG; GR1540/20-1). KWT was further supported by a Humboldt Research Fellowship.

*Submitted 27 May 2015*

*Revised 14 July 2015*

*Accepted 16 July 2015*

*Associate editor: Maren Voss*